MATERIALS CHEMISTRY FRONTIERS

RESEARCH ARTICLE

View Article Online
View Journal | View Issue

Cite this: *Mater. Chem. Front.*, 2025, **9**, 2770

Panchromatic photochromic push–pull dyes featuring a ferrocene donor group

Diego Mirani, * Antonio J. Riquelme, Samuel Fauvel, Cyril Aumaître, Pascale Maldivi, Jacques Pécaut and Renaud Demadrille *

Photochromic molecules are light-responsive compounds that undergo reversible structural changes when exposed to light, producing isomers with different absorption spectra. Their ability to switch between molecular states with different optical properties makes them valuable for use in smart materials, anti-counterfeiting systems, optical data storage and optoelectronic devices. Diphenyl-naphthopyrans are a type of photochromic system that has attracted particular interest due to their tunable absorption spectra, fast response times and good fatigue resistance. However, their relatively narrow and selective absorption in the visible spectrum limits their use in applications requiring neutral colouration, such as smart windows and ophthalmic lenses. To address this limitation, we investigated which structural modifications could be employed to adjust the key optical and photochromic properties, such as the absorption range, colouring ability, and isomerisation kinetics. In this study, we present a strategy for obtaining novel push–pull photochromic dyes with wide, panchromatic absorption. Our approach involves replacing a phenyl unit with a ferrocene unit within the diphenyl-naphthopyran framework, while also adding an anchoring acceptor group to create a push–pull structure. We present the synthesis of five new dyes, detailing their optical and electrochemical properties. We investigated their photochromic behaviour in both solution and the solid state by grafting them onto metal oxide surfaces or dispersing them in a polymer matrix. Our results demonstrate that these dyes can be used to effectively produce panchromatic photochromic coatings. Furthermore, we show that some of these compounds act as efficient photosensitisers in dye-sensitised solar cells (DSSCs).

Received 5th June 2025,
Accepted 5th August 2025

DOI: 10.1039/d5qm00412h

rsc.li/frontiers-materials

Introduction

Photochromic dyes are a unique class of compounds that reversibly change colour when exposed to light. These molecules can undergo reversible isomerisation when they absorb a photon and the photogenerated isomer shows different optical properties.[1] The phenomenon of photochromism was first observed in the 19th century by Fritzsche, who noticed light-induced colour changes in certain compounds and nowadays photochromic materials have found applications for example in optical memory,[2–4] neuromorphic models,[5] sensors,[6–8] smart windows,[9,10] optoelectronics,[11] surface coatings,[12] anti-counterfeiting systems,[13,14] optical lenses for ophthalmology,[15–19] and photovoltaic devices.[20–22] Their ability to switch between multiple distinct states with different absorption spectra and energy levels makes them ideal for dynamic and adaptive applications, including nonlinear optics and molecular electronics.[23]

There are several classes of photochromic molecules, each with a different isomerisation process, properties and potential applications. These compounds can be broadly classified into P-type and T-type photochromes based on their reversibility mechanisms.[15] P-type photochromes, such as diarylethenes[11,24] and fulgides,[25] exhibit a thermally stable coloured state after photoisomerization, requiring a specific light stimulus to revert to their original form. In contrast, T-type photochromes, including azobenzenes,[26,27] spiropyrans,[28] spirooxazines,[3] and diaryl-naphthopyrans,[29] undergo spontaneous thermal relaxation, and return to their original state without the need for additional light exposure.

Photochromic molecules work through a photo-induced structural change that alters their electronic configuration and, consequently, their optical absorption. This transformation typically involves processes such as pericyclic reactions, *cis–trans* isomerisations, tautomeric shifts, or electron transfer mechanisms, depending on the chemical structure of the molecule.[15] The efficiency of this reversible reaction is an important factor determining the potential of photochromic materials in various applications. In addition, fatigue resistance, such as the ability to withstand multiple switching cycles without degradation, photostability under continuous irradiation and response time corresponding to the speed of colour change, play a crucial role in the selection of suitable photochromic compounds for specific applications. Among the various photochromes, diphenyl-

Univ. Grenoble Alpes, CEA, CNRS, Gre-INP, IRIG-SyMMES, 38000 Grenoble, France. E-mail: renaud.demadrille@cea.fr

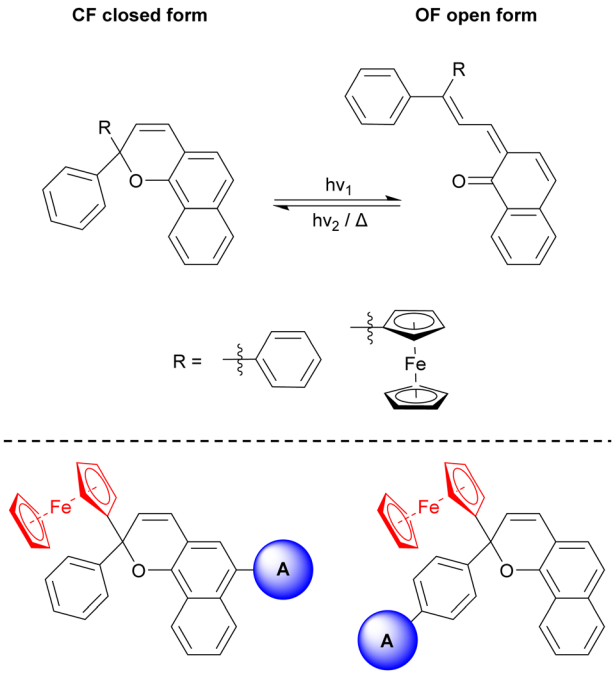

Fig. 1 Photo-induced reversible isomerization process in diphenyl-naphthopyran molecules between the closed form (CF) and the open form (OF) the molecules with and without ferrocene modification are represented. Below, naphthopyran dyes with a ferrocene group and presenting also an acceptor moiety (A) in different geometries.

naphthopyrans are between the most commercially important due to their tunable structures and wide colour range, making them ideal for applications such as ophthalmic lenses, coatings, and smart materials. Their photochromic process relies on a transition between a colorless closed form (CF), and multiple colourful open form (OF) (Fig. 1). When irradiated with near UV light, a ring-opening mechanism is induced, producing the fully conjugated species responsible for the coloured state, while thermal or visible light exposure restores the original colourless form. Structural modifications allow fine-tuning of absorption maxima, response speed, and thermal stability. Additionally, some naphthopyrans exhibit good fatigue resistance, ensuring long-term photochromic performance in consumer applications.[15,29,30]

The optical properties of photochromic molecules are primarily defined by their colourability (the intensity and range of colours produced) and the kinetics of discoloration (the speed at which they revert to their original colourless state). Precise molecular design allows the photochromic properties, in particular the absorption spectra and the rate of colouration and decolouration,[31,32] to be fine-tuned to suit the application.[19,29,33–35]

Considering applications like transparent coatings and ophthalmology, the colour of the dye in the active form is of primary importance. To reduce colour distortion through a photochromic semi-transparent material, the incorporated dyes should have a neutral coloration, hence a panchromatic absorption, as flat as possible over the visible range. Achieving this condition using diphenyl-naphthopyran molecules was only possible by combining two dyes with complementary absorption.[16,36] However, mixing two dyes the system gains in complexity and it is often difficult to match the properties like the kinetic of coloration and discoloration of the different photochromes.[37] The literature on diphenyl-naphthopyran dyes with broad absorption in the visible is scarce. Only a few patents report that, by appropriate molecular engineering, it is possible to introduce functional groups on the photochromic core, allowing a coloured form with two broad absorption bands in the visible, leading in some cases to almost neutral shades with a single dye.[38,39]

Another strategy to broaden the absorption of photochromic dyes in the visible range, was introduced by Anguille and co-workers in 1998. Their approach was based on the introduction of a ferrocenyl unit to the naphthopyran photochromic moiety (Fig. 1).[40–42] By replacing one of the phenyl groups in a diphenyl-naphthopyran structure with a ferrocene, two absorption bands were observed in the open form spectrum of the molecule, resulting in a broader absorption across the visible range and a neutral colour (Fig. S1[40]). However, the origin of this phenomenon and the appearance of a second transition was not elucidated.

The implementation of ferrocenyl moiety in push–pull non-photochromic dyes was previously investigated due to the stable redox properties of this unit. Numerous dyes were developed and investigated in the last years, notably for application in DSSCs. In these dyes, the ferrocenyl unit is usually used as the electron donor unit in the photosensitizers.[43–57] One can note that ferrocene was also used in DSSCs as the redox mediator in liquid electrolytes[58,59] due to its stable redox properties and versatile oxidation state of the iron in the complex (Fe^{3+}/Fe^{2+}). By implementing DFT modelling, these studies were able to show that, when coupling the metallocene group with an acceptor moiety, it is indeed possible to have a HOMO level electronic density mostly located on the ferrocene, hence a good donor character in this position. The formation of an additional absorption band is also often observed in non-photochromic dyes embedding a ferrocene unit and often attributed to an intramolecular charge transfer (ICT) transition between the ferrocenyl unit and the acceptor, where the LUMO is located.[43,50,51,56,57]

The use of a push–pull chemical structure in photochromic dyes is a well-established strategy to shift the absorption maximum of the molecule (after photoconversion) toward the visible region. In addition, ferrocene units have been shown to broaden the absorption spectrum due to additional electronic transitions.[40] In this work, we combined both approaches by incorporating a ferrocenyl group as the electron-donating unit in the push–pull system of our photochromic dyes. The expected outcome of our strategy was to obtain panchromatic photochromic dyes and to exploit the redox properties of ferrocene for a potential application in photovoltaic devices. We decide to replace one phenyl unit by a ferrocene moiety and given the non-symmetric nature of the photochromic core, two different options can be proposed, one where the acceptor and anchoring function is linked on the naphthol part, and a second where it is linked to the remaining phenyl group (Fig. 1).

When considering applications in photochromic coatings for use in ophthalmic lenses, we decided to characterize the optical properties of the dyes not only in solution as it is commonly done but also in a polymer matrix. The introduction of photochromic dyes in polymeric matrices[60] or sol–gel matrices[61] have been extensively reported.[62–64] Based on the research performed on the subject, we study the implementation of the most promising dye in poly-methyl methacrylate (PMMA) matrices, as it is one of the most relevant materials to be studied with photochromic molecules,[65] and studied the optical properties.

Given that the acceptor part includes an anchoring function, the possibility to test the dyes in photochromic dye-sensitized solar cells is also investigated. These multifunctional solar cells have been recently developed[21] and several examples of photochromic dyes from the diphenyl naphthopyran family have been reported for use in these devices.[22,66,67] A key challenge in using photochromic dyes for semi-transparent solar cells is their narrow absorption range, which leads to specific colouration that can distort visibility and limit their use in glazing. The development and integration of panchromatic photochromic dyes offers a promising solution, advancing the path towards panchromatic photochromic dye-sensitised solar cells.

Results and discussion

Design and synthesis of the molecules

Based on the dye structure developed and studied by Anguille *et al.*,[40] we have designed dyes that contain a strong mesomeric electron acceptor moiety embedding a carbonyl group that allows it to be anchored to the surface of metal oxides through surface esters.[68] We started by using density functional theory (DFT) to calculate the distribution of orbitals and energy levels for dyes with different structures embedding a donor ferrocene and the electron accepting unit. If these dyes are to be used in dye solar cells the HOMO level of the dyes must be below the reduction potential of the redox couple making up the electrolyte and their LUMO must be above the conduction band of the electrode. This means HOMO below −4.8 eV for iodine-based electrolytes and LUMO above −4.1 eV for TiO_2 based electrode.[69] The results of the modelling will be discussed below together with the results of the cyclic voltammetry measurements. After extensive research and modelling of more than 20 different compounds, five structures were identified as valuable for applications and could be readily synthesised for further study (Scheme 1). The first three structures have the donor (ferrocene) and acceptor on opposite sides of the π-conjugated system, while the other two are on the same side of the photochromic moiety. The identified structures that meet the energetic requirements of the dyes to be used as photosensitisers are detailed below. In **DiMi-1**, a cyanoacetic acid acceptor group is attached to the naphthalene of the naphthopyran moiety by a phenyl spacer. In **DiMi-2** a thiophene group is used as spacer providing a more planar connection between the anchoring group and the rest of the molecule.[70] To develop **DiMi-3** we used a more complex naphthopyran core with an indeno bridge that is known to speed up the kinetic of discoloration of the dye.[22] With **DiMi-4** and **DiMi-5**, we wanted to investigate a completely new design with the anchoring function attached to the remaining phenyl of the photochromic core, the two dyes have the same structure, the only difference lies in the presence of two methyl groups in the **DiMi-5** structure that are introduced to speed up the discoloration of the dye by hindering the open form.

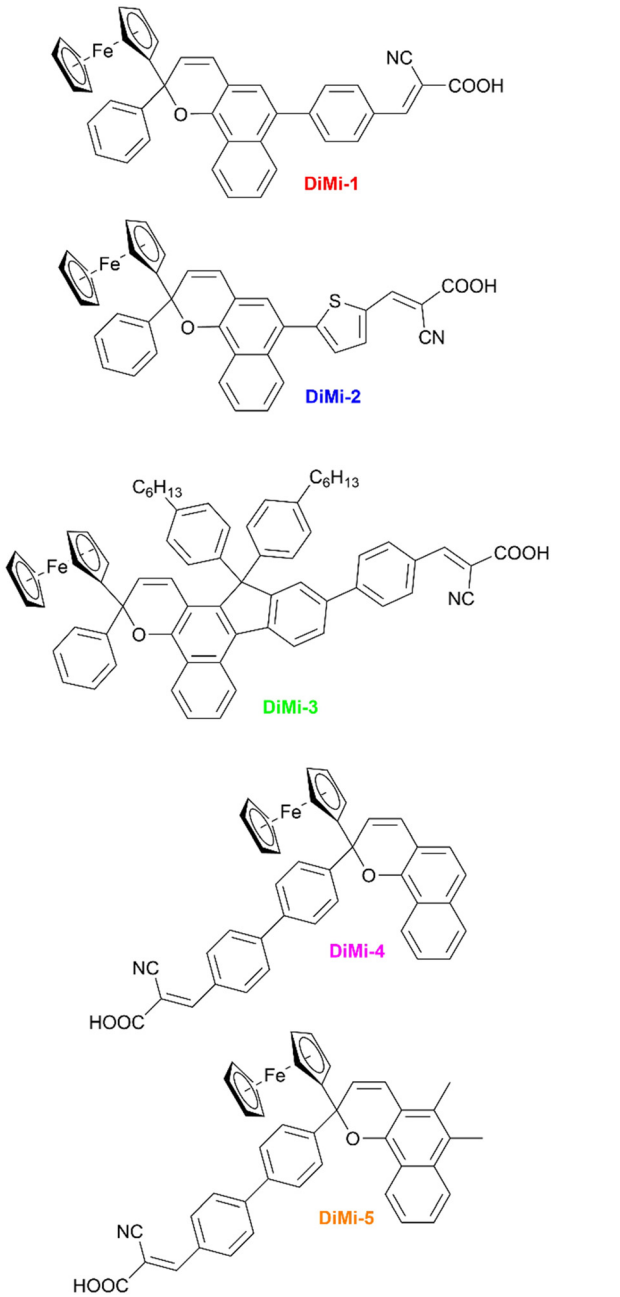

Scheme 1 Structures of the synthesized photochromic dyes in the closed form: **DiMi-1** (with phenyl spacer); **DiMi-2** (with thiophene spacer); **DiMi-3** (with indeno bridge spacer); **DiMi-4** (with inverted structure) and **DiMi-5** (with inverted structure and methyl groups).

In the case of **DiMi-1**, **DiMi-2** and **DiMi-3** (Scheme 2) the synthesis starts with the preparation of the different naphthols specific to each dye. Suzuki–Miyaura coupling reaction of 4-bromo-1-naphthol with either 4-formylphenylboronic acid

or 5-formyl-2-thienylboronic acid gives **1** and **3** respectively. Low yields were observed most likely due to aldehyde interaction with the catalyst and the use of non-protected boronic acids. The protected naphthol core of **DiMi-3** was synthesized following a previously reported procedure in the literature,[22] and its deprotection using boron tribromide gave the naphthol **5** with good yield. 1-Ferrocenyl-1-phenyl-2-propyn-1-ol (**Prec1**) was synthesized following a previously reported procedure in

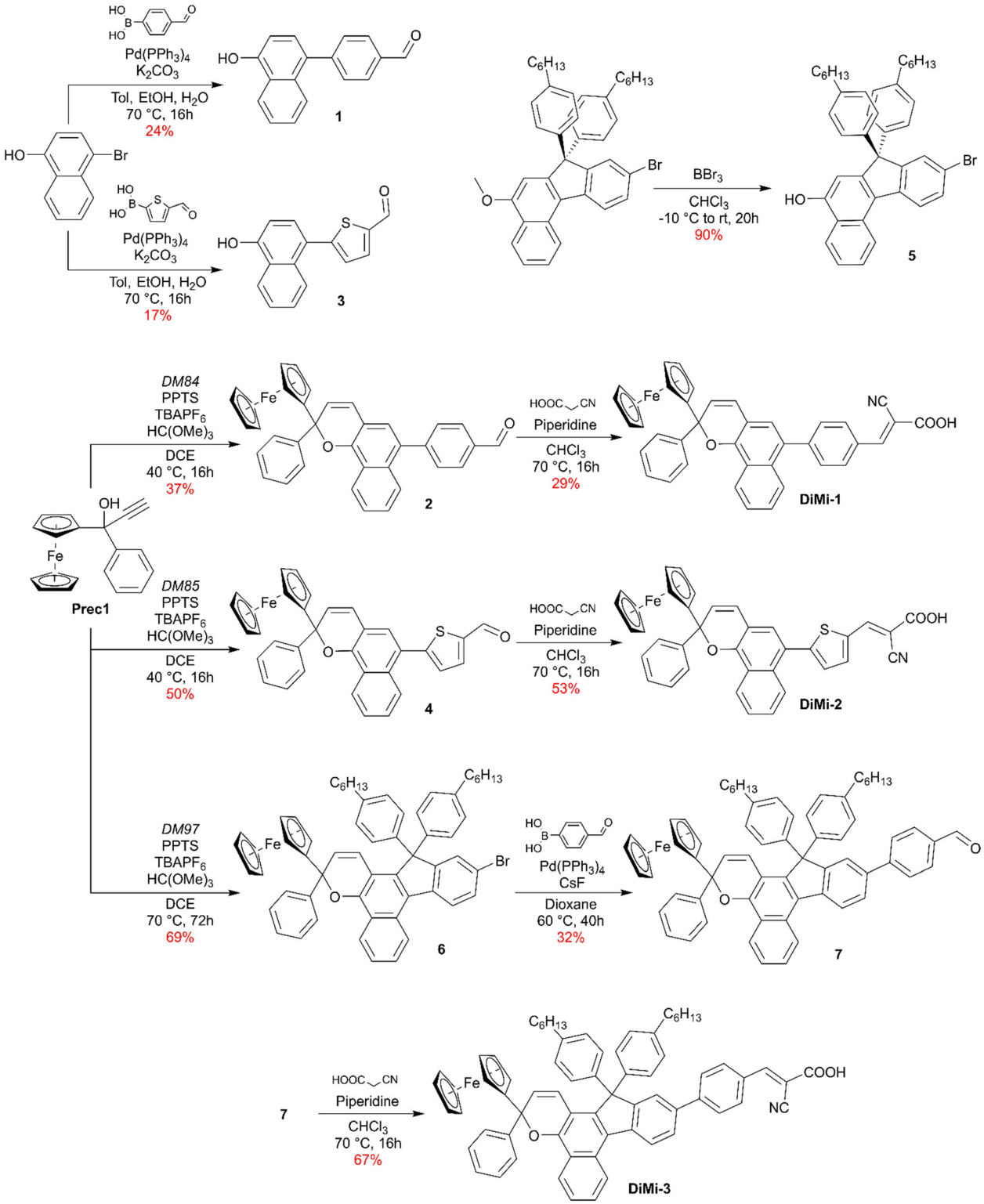

Scheme 2 Synthetic route for the dyes **DiMi-1**, **DiMi-2** and **DiMi-3**.

the literature[40] and the chromenisation reaction with the deprotected naphthols previously synthesized gave **2**, **4** and **6** as photochromic molecules. Another Suzuki–Miyaura coupling reaction on the latter product with 4-formylphenylboronic acid gave **7**. Finally, all the aldehydes intermediates were reacted with cyanoacrylic acid to yield the final photochromic dyes.

In the case of **DiMi-4** and **DiMi-5** (Scheme 3) the synthesis starts with the preparation of the brominated ferrocenyl propargyl alcohol by Friedel–Crafts acylation on ferrocene with 4-bromobenzoyl chloride to obtain **8**. Then lithiated trimethylsilylacetylene is used for a nucleophilic attack on the ketone to yield **9** after alkaline workup. A chromenisation reaction between the propargyl alcohol and either 1-naphthol or 3,4-dimethyl-1-naphthol (synthesized following a previously reported procedure in literature[42]) yielded respectively **10** and **12**. Suzuki–Miyaura coupling reaction was performed on both the compounds with 4-formylphenylboronic acid to obtain respectively **11** and **13**. And lastly the aldehydes intermediates were employed in a Knoevenagel condensation with cyano-acrylic acid to yield the final photochromic dyes. Single-crystal X-ray diffraction analysis was performed for a selection of the synthesized compounds. Key crystallographic data and full structural details are provided as SI. Crystallographic data for the structural analysis have been deposited with the Cambridge Crystallographic Data Centre, no. CCDC-2455768 (**Prec1**), CCDC-2455765 (**1**), CCDC-2455769 (**3**), CCDC-2455771 (**8**), CCDC-2455767 (**9**), CCDC-2455770 (**10**), CCDC-2455773 (**11**), CCDC-2455772 (**12**) and CCDC-2455766 (**13**).

Optical characterization

The optical properties of the molecules, such as UV-visible absorption spectra before and after irradiation and thermal discolouration kinetics between the open and closed forms, have been extensively studied. Absorption spectra are measured on toluene solutions before and after irradiation with a broad-

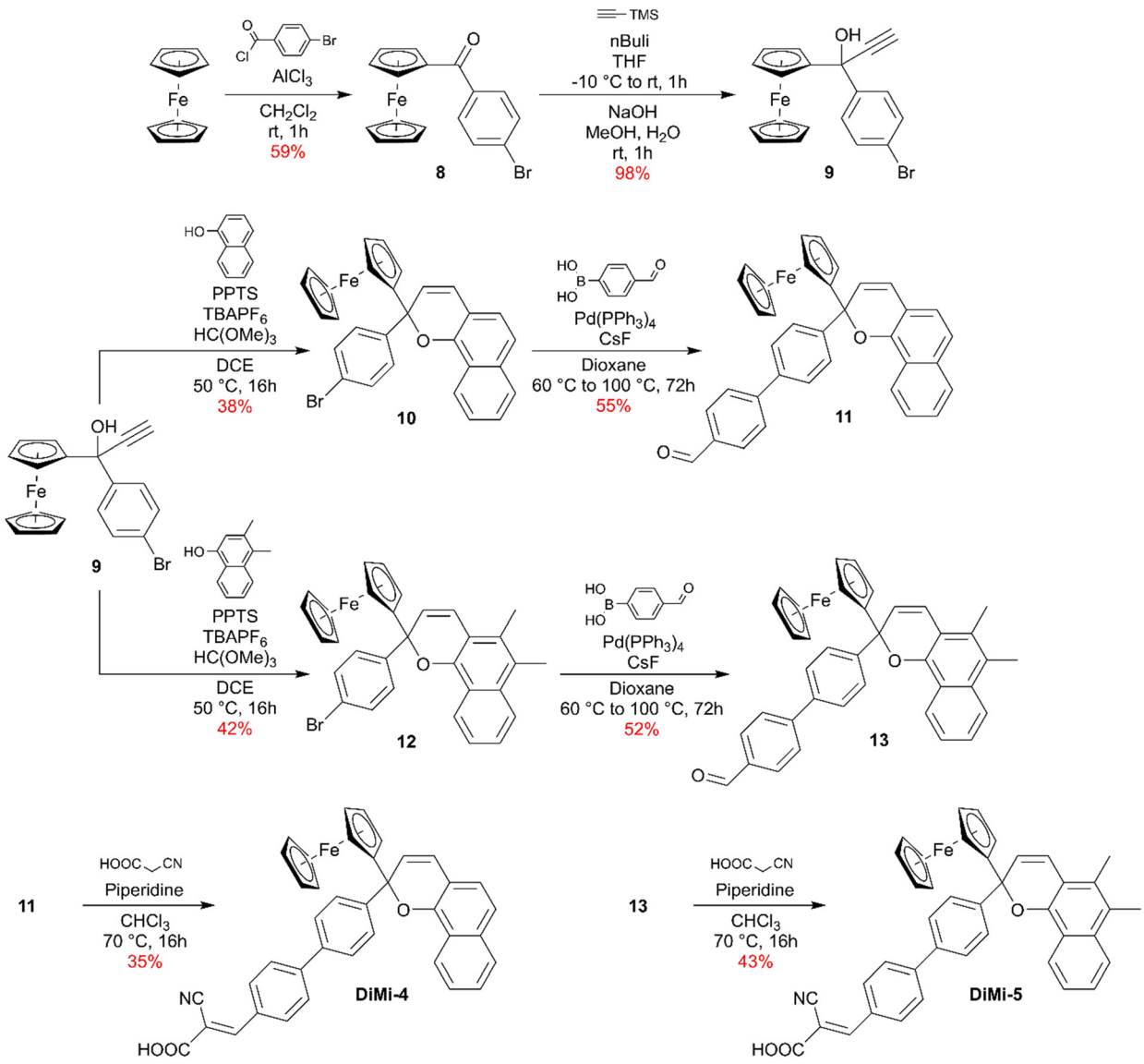

Scheme 3 Synthetic route for the dyes **DiMi-4** and **DiMi-5**.

beam (250–1050 nm, 300 W) lamp for about 5 minutes or until the photostationary state (PSS) is reached. The photostationary state corresponds to the thermodynamic equilibrium between the closed and open isomers under constant illumination.[71,72]

In agreement with literature examples on diphenyl-naphthopyrans, all the synthesised dyes show photochromic behaviour upon polychromatic irradiation (Fig. 2). **DiMi-2** and **DiMi-3** show a yellowish colour in solution before irradiation, whereas the other dyes are uncoloured. Under illumination, as expected, the introduction of the ferrocene moiety induces a broad absorption over the visible range and the formation of a second absorption band is observed in the OF, specifically for the dyes **DiMi-1**, **DiMi-4**, and **DiMi-5**. These dyes in solution show a quasi-neutral coloration close to grey-beige when observed with the naked eye. All the dyes exhibit extended absorption, ranging from the UV region up to 740 nm for **DiMi-4** and **DiMi-5**, and reaching the edge of the NIR region at 800 nm for the other three molecules, confirming their panchromatic absorption. It should be noted that the replacement of the phenyl spacer in **DiMi-1** by a thiophene in **DiMi-2** has the effect of bathochromically shifting the spectrum of the closed and open forms, as does the extension with the indene unit in **DiMi-3**. On the other hand, positioning the acceptor function on the ferrocene side maintains the absorption of the closed form in the UV and limits the absorption of the open form below 750 nm for **DiMi-4** and **DiMi-5**.

Time-dependent DFT (TD-DFT) calculations were carried out to simulate the electronic absorption spectra and aid in the assignment of the observed experimental bands. Among these, B3LYP functional showed the best agreement with the experimental data and was therefore used for further analysis (see SI for more details). This theoretical approach allowed us to attribute the additional absorption bands observed experimentally (see SI and Fig. S2). Full computational details are provided in the SI. For each dye, the three most important excitations, in terms of oscillator strength are studied. The results show that for all the dyes the transition at lowest energy (HOMO to LUMO) intervenes mainly on the π system leading to a displacement of the charge upon excitation from the donor to the acceptor, typical of push–pull dyes. The second excitation in terms of energy shows for **DiMi-1** and **DiMi-2** strong participation from the ferrocene orbitals, confirming their role in the absorption. Similar to what was observed previously, **DiMi-5** exhibits the same behaviour with lower intensity. For **DiMi-3** and **DiMi-4** contribution of the ferrocene in this excitation is less evident. The third analysed excitation falls at higher energies and is located on the π system leading to the absorption that we can observe in the CF of the molecules. Although TD-DFT predicts a high oscillator strength for the transition of the open form, enabling qualitative assignment, a quantitative comparison with experimental data is not feasible due to the photostationary state (PSS) being an equilibrium mixture of closed and open forms.

After reaching the PSS, the irradiation source was turned off, and we study the evolution of the characteristic absorption peak of the OF for each molecule over time to obtain the thermal discoloration curves. An exponential regression is then applied to the absorption data over time, using either a single or double exponential fit, depending on the experimental results:

$$A(t) = a_1 e^{-k_1 t} + A_\infty; \quad A(t) = a_1 e^{-k_1 t} + a_2 e^{-k_2 t} + A_\infty$$

where $A(t)$ represents the absorbance of the solution, k_n is the thermal discoloration kinetic constant (s^{-1}), a_n denotes the

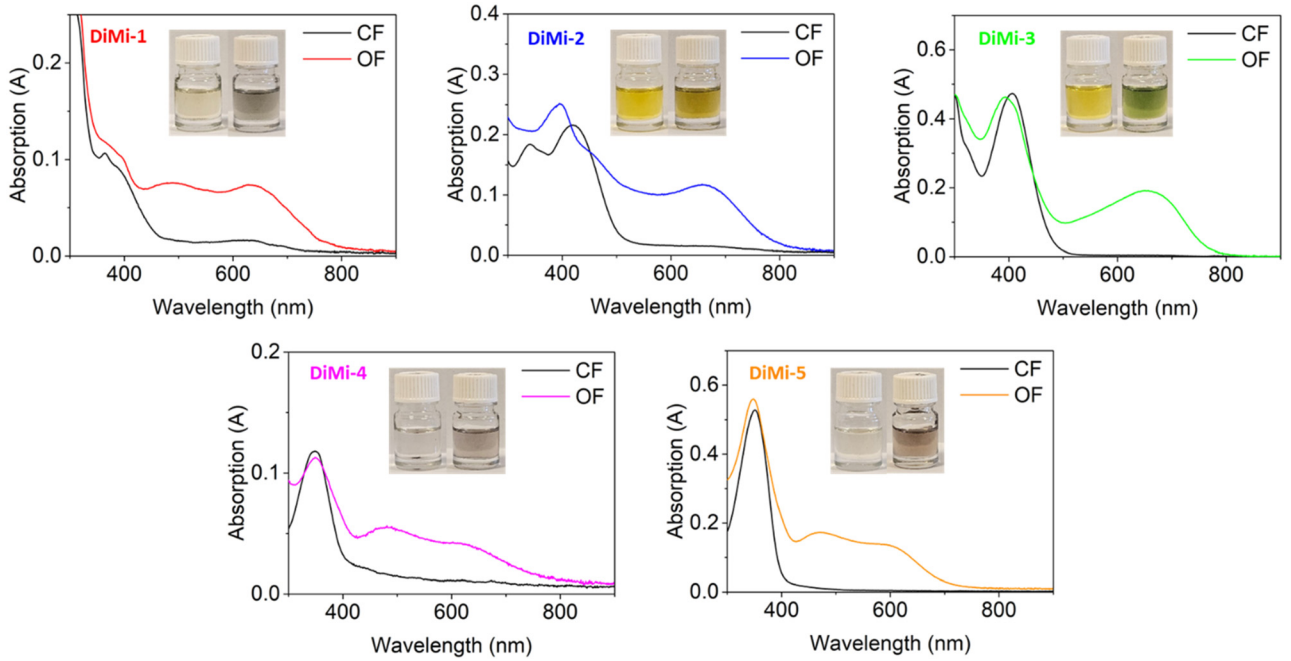

Fig. 2 UV-visible absorption spectra of the described dyes (2×10^{-5} M in toluene, 25 °C) before irradiation (black curves) and after reaching the PSS with continuous irradiation with a polychromatic lamp (coloured curves).

amplitude of the kinetic process, and A_∞ is the residual absorbance.

The optical data and photochromic properties including the kinetics of discoloration are shown in Fig. 3 and summarized in Table 1. From the absorption measured at the photostationary state (PSS), the colourability (C_λ) of the dye is calculated as the maximum visible-range absorbance under illumination divided by the initial concentration of the dye in solution. This value represents an apparent molar absorption coefficient, since the exact fraction of the open (colored) form at PSS is unknown. It should therefore be considered an approximation for comparative purposes between dyes under identical conditions.

All photochromic molecules show reversible colouring behaviour. **DiMi-2**, **DiMi-3** and **DiMi-5** show the highest colourability (A_0) under these conditions, this corresponds to the absorption at the PSS. Compared to **DiMi-1**, we observed that the introduction of the thiophene spacer in **DiMi-2** leads to a faster decolouration process. However, as expected, the greater effect on the kinetics is observed when the dyes are more hindered in the open form (**DiMi-3** and **DiMi-5**). The introduction of a highly sterically hindered group, such as the indeno moiety in **DiMi-3**, results in a decolouration process following a mono exponential decay.

These results, which confirm a photochromic behaviour associated with panchromatic absorption, encourage further characterisation of the dyes in the solid state in view of the potential applications outlined in the introduction.

Study in polymeric matrix

As the optical properties of the dyes, related to their photochromism and neutral colouration, are quite outstanding in solution, the potential for solid state applications is being investigated. For the purpose of this study, we focused on **DiMi-5** that shows a good equilibrium between the flat absorption with neutral coloration and fast kinetics of discoloration. Its optical behaviour is studied by dispersion in a polymeric matrix based on poly(methyl-methacrylate) (PMMA) very often used to study isomerization of photochromic dyes.[64,73]

The results, in Fig. 4, show that a homogeneous polymer/dye matrix with a slightly yellow coloration is obtained. The matrix is then irradiated with a UV light for 20 minutes. During this process a logo mask was positioned on the film. The results show that after irradiation, a color change is observed as the logo shows through the film (Fig. 4) this means that the dye goes through isomerization to the OF. If the irradiated film is left in the dark overnight, the OF reverts to the CF with the film discolouring to the initial state. The photochromic behaviour is tested again on the same film and, by keeping the matrix at 30 °C in the dark we observe a decolouration to the initial state in 2 hours. The UV-vis absorption spectrum of the film is also measured (Fig. S3A) and the results show that after irradiation a coloration with flat absorption typical of **DiMi-5** is observed. Calculation of AVT and CRI values of the polymeric matrix before and after irradiation allowed us to verify that upon colouration the AVT value changes from 91% to 86% and the CRI value remains at 99, showing indeed a photochromic panchromatic response to the absorption.

Additionally, this activation of the dye reverts after keeping the matrix in the dark to complete discoloration. Lastly, the discoloration kinetics of the film (Fig. S3B), it is observed that the dye dispersed in the film reverts more slowly than the dye in solution, while still maintaining a relatively fast response.

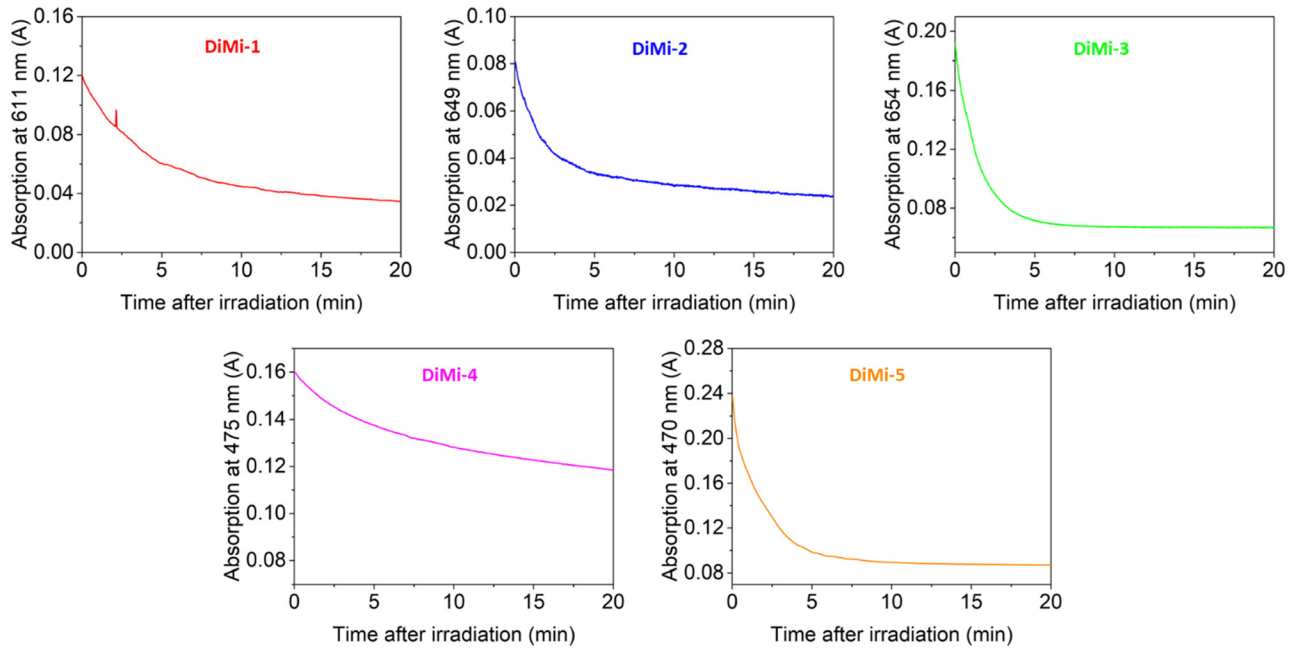

Fig. 3 Discoloration curves of the described dyes in solution (2×10^{-5} M in toluene, 25 °C) in the dark after the PSS was reached under irradiation with polychromatic light. For each dye a wavelength representative of the difference between the OF and CF was monitored (611 nm) for **DiMi-1**, 649 nm for **DiMi-2**, 654 nm for **DiMi-3**, 475 nm for **DiMi-4** and 470 nm for **DiMi-5**.

Table 1 Optical parameters of the described dyes obtain with 2×10^{-5} M solutions in toluene at 25 °C

Dye	Form	λ_{max} (nm)	λ_{onset} (nm)	C_λ (L mol^{-1} cm^{-1})	a_1	k_1 (s^{-1})	a_2	k_2 (s^{-1})
DiMi-1	CF	365	458	3700 (at 632 nm)	0.075	3.9×10^{-3}	0.037	2.1×10^{-4}
	OF	365, 477, 632	766					
DiMi-2	CF	425	500	5900 (at 657 nm)	0.046	8.6×10^{-3}	0.025	2.9×10^{-4}
	OF	400, 657	778					
DiMi-3	CF	413	479	9600 (at 655 nm)	0.122	8.6×10^{-2}	—	—
	OF	401, 655	754					
DiMi-4	CF	350	397	2100 (at 606 nm)	0.029	2.0×10^{-3}	0.043	2.5×10^{-4}
	OF	352, 469, 606	724					
DiMi-5	CF	351	396	6800 (at 597 nm)	0.025	1.2×10^{-1}	0.129	7.7×10^{-3}
	OF	350, 469, 597	693					

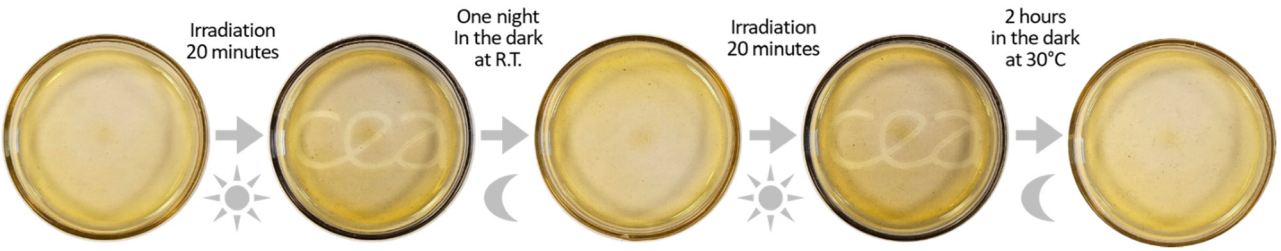

Fig. 4 Polymeric matrix based on PMMA and containing **DiMi-5**, before irradiation, after irradiation and after deactivation in the dark.

This proves that the molecule can be photochromic while being suspended in a polymeric matrix obtaining photochromic panchromatic films.

Study onto mesoporous TiO_2 layers

Another way to investigate the optical properties of the synthesized molecule in the solid state was to graft them on a mesoporous electrode through their acidic anchoring function and study the behaviour before and after irradiation. Five TiO_2 electrodes were dipped overnight in dyeing bath of the different molecules, were irradiated under a wide-emission lamp (containing UV) and then were left in the dark for five days.

Although a low colourability was measured in solution, examining the coloration behaviour of the sensitized electrodes (Fig. 5) allows us to distinguish two categories of dyes. Once grafted onto a mesoporous TiO_2 electrode, the photochromic response is notably altered for certain dyes, indicating that the solid-state environment significantly influences their switching behaviour. **DiMi-1**, **DiMi-2** and **DiMi-4** give very coloured electrodes before irradiation, indicating that the molecules open up in the dye bath at the time of grafting and do not close again once attached. Only a slight change is observed after irradiation. On the contrary, **DiMi-3** and **DiMi-5**, the molecules with the fastest decolourisation kinetics, retain their photochromic behaviour after grafting. The electrodes, although initially coloured due to an absorption edge in the visible for the closed form, coloured under irradiation and slowly faded over several days in the dark. Slower kinetics are a known phenomenon for this family of photochromes once they have been grafted, and this is due to the strong steric interactions between the molecules that stabilizes the open form and prevent ring closure.[21] Despite the strong impact of grafting on the photochromic properties, we decided to investigate the potential of the dyes as sensitizers in DSSC configuration.

Electrochemical characterization

Before implementing these molecules in DSSCs, their compatibility with other components, in particular the TiO_2 electrode and the iodine-based redox mediator, must be evaluated. The photochromic dyes should have LUMO levels higher than the conduction band of TiO_2 to enable efficient electron injection and HOMO levels lower than the reduction potential of the iodine-based electrolyte to ensure effective dye regeneration.

The HOMO and LUMO levels for the closed and open forms are determined using cyclic voltammetry and UV-vis absorption spectroscopy. Cyclic voltammetry experiments were performed on solutions of the dyes in dichloromethane to determine the HOMO level of the molecules (Fig. S4 and S5). The HOMO level is determined before and after irradiation to study the CF and OF respectively. The LUMO level is determined by adding the energy of the band gap determined with the UV-vis absorption technique to the HOMO. Although this method is not the most accurate, it allows us to compare the values with those obtained by DFT and to check that the energy levels of the dye are compatible with the other components of the solar cells and that the experimental values are in agreement with the

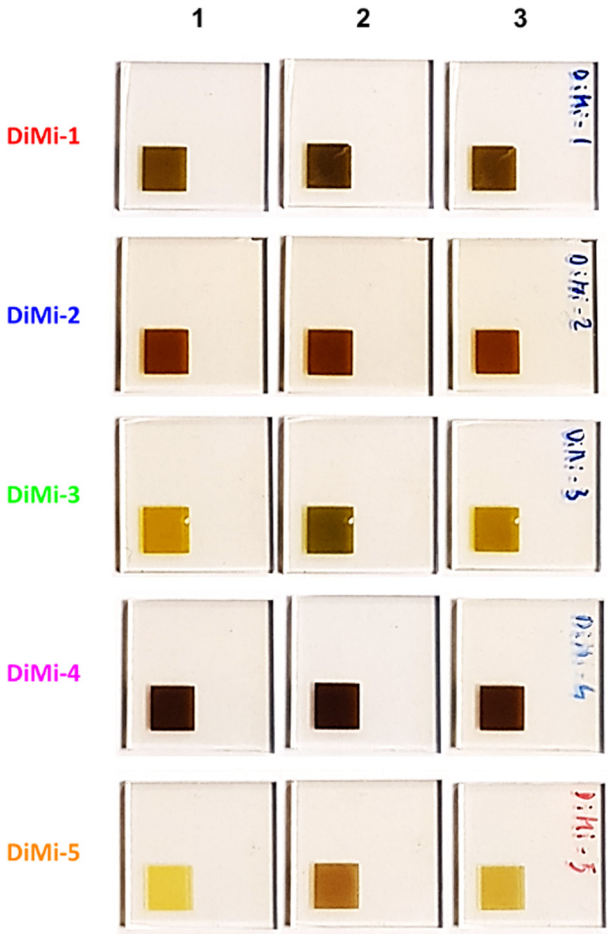

Fig. 5 TiO_2 electrodes grafted with the synthesized dyes. (1) Before irradiation, (2) after irradiation and (3) after five days in the dark.

theoretical values. The results together with the theoretical ones obtain through DFT calculations are reported in Fig. 6.

Study in solar cells

Since the dyes can be grafted onto mesoporous TiO_2 layers and have energy levels compatible for use in DSSCs, their photovoltaic performance is evaluated in semi-transparent solar cells. Although some of the dyes lose their photochromic behaviour once they are grafted onto the electrodes, it is important to measure their performance in order to compare them with other ferrocene pattern photosensitisers reported in the literature. Two types of electrolytes were used to fabricate the DSSCs, a home-made electrolyte[21] specifically designed for photochromic naphthopyran dyes (Acetonitrile, 0.09 M I_2, 0.5 M LiI) and an electrolyte with lower content of iodine, used for DSSCs containing ferrocenyl-based dyes (acetonitrile, 0.05 M I_2, 0.1 M LiI, 0.5 M TBP, 0.6 M DMPII).[51,53,54,57] For each conditions two cells were prepared using semitransparent TiO_2 mesoporous electrodes of 8 μm thickness, and a dying bath using a ratio of 1 : 10 dye/CDCA (Chenodeoxycholic acid) as a co-absorbent, this ratio is typically chosen to achieve an effective balance between high dye loading and suppression of aggregation. The obtained cells are then characterized performing JV measurements in a solar simulator AM 1.5G (1000 W m^{-2}) to determine the performance in terms of V_{oc}, J_{sc}, FF and PCE (power conversion efficiency). The cells are measured before and after light soaking to study the evolution of the performance while activating the photochromic dyes.

The results in terms of photovoltaic performance are shown in Table 2 and correspond to the measurements after few tens of seconds under irradiation. After prolonged irradiation, however not all the dyes are stable and the performance of the corresponding DSSCs decrease progressively for some of them.

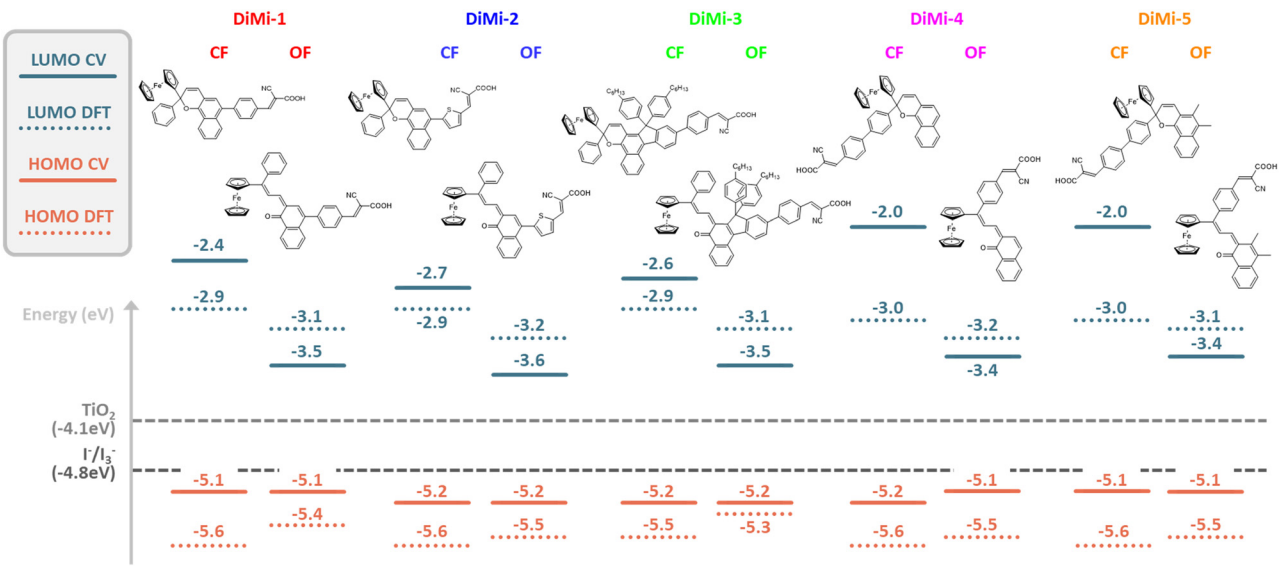

Fig. 6 Theoretical and experimental HOMO and LUMO energy levels of the closed and open form of each dye. The experimental HOMO is calculated through cyclic voltammetry (2×10^{-3} M in DCM/$TBAPF_6$ 0.1 M), the experimental LUMO by determination of band-gap energy through absorption spectroscopy (2×10^{-3} M in toluene) and addition to HOMO energy. The theoretical energy levels are determined from a single-point modelling using B3LYP hybrid functional (more details in SI). The positions of the conduction band of TiO_2 and the reduction potential of the iodine-based redox couple are indicated with horizontal dashed lines.

Table 2 Performance in terms of PCE (%) for the described dyes before light soaking. Best performance and average in parenthesis. Two different electrolyte compositions are studied: iodine (acetonitrile, 0.09 M I_2, 0.5 M LiI); low concentration iodine (acetonitrile, 0.05 M I_2, 0.1 M LiI, 0.5 M TBP, 0.6 M DMPII). At least two cells for each condition

Dye	Electrolyte	V_{oc} (mV)	J_{sc} (mA cm^{-2})	FF (%)	PCE (%)
DiMi-1	Iodine	476 (482)	2.66 (2.60)	63 (63)	0.80 (0.79)
	Low conc. iodine	627 (627)	2.42 (2.34)	75 (76)	1.15 (1.12)
DiMi-2	Iodine	454 (467)	5.39 (4.44)	60 (61)	1.47 (1.25)
	Low conc. iodine	604 (603)	2.99 (3.00)	77 (76)	1.40 (1.37)
DiMi-3	Iodine	458 (449)	7.02 (6.82)	59 (56)	1.91 (1.73)
	Low conc. iodine	677 (688)	4.25 (3.95)	78 (72)	2.23 (1.97)
DiMi-4	Iodine	334 (334)	1.40 (1.40)	64 (63)	0.30 (0.29)
	Low conc. iodine	540 (532)	0.52 (0.49)	70 (72)	0.20 (0.19)
DiMi-5	Iodine	405 (407)	1.95 (1.75)	57 (58)	0.45 (0.42)
	Low conc. iodine	599 (567)	0.88 (0.66)	65 (68)	0.34 (0.25)

This instability could be explained by the formation of ferricenium iodide ion-pair under illumination,[74] which interfere with the regeneration mechanism of the dyes. In addition, we found that all the dyes lose their photochromic behaviour in a complete DSSC configuration, but they retain their photosensitising behaviour absorbing light and converting it into electricity. Nevertheless, the dyes **DiMi-1**, **DiMi-2** and **DiMi-3** still show the best photovoltaic properties after light irradiation with PCE ranging from *circa* 1% to 2.2%. Although the results obtained with these dyes are low, they are comparable and even sometimes superior to other ferrocene-based dyes reported in the literature.[57,75]

Lastly, to additionally verify the behaviour of the dye in the device under light irradiation the solar cells fabrication process was repeated on 16 cm^2 electrodes using **DiMi-5** and an electrolyte with reduced concentration in iodine (Acetonitrile, 0.009 M I_2, 0.05 M LiI). As expected, the PCE was below 1% and no substantial change in coloration after 10 minutes irradiation was noticed, however a neutral coloration was observed with an AVT of 64% and a CRI of 94 (Fig. S6).

Conclusion

In this study, the incorporation of a ferrocenyl donor unit into push–pull photochromic dyes was investigated with the aim of enriching their photochromic optical properties with panchromatic absorption. Five molecules with different properties were designed, modelled and synthesised. Their optical properties were studied in solution and showed photochromic behaviour with panchromatic absorption in the activated form. Similar optical properties were also observed when the dyes were embedded in a polymer matrix.

The potential application of the synthesized dyes in dye-sensitised solar cells (DSSCs) was investigated by evaluating the electronic compatibility of their HOMO and LUMO energy levels with the other components of the solar cell, as well as by assessing their optical behaviour on bare electrodes. Despite the energy compatibility of the dyes for use in DSSCs, we observed a loss of photochromic properties once attached to the electrodes in the complete cell. The solar cells obtained show performances comparable to the state of the art of other dyes containing a ferrocene unit, but poor stability.

This study is the first to investigate the implementation of the ferrocenyl moiety in push–pull photochromic dyes, providing new insights into panchromatic photochromic molecules with redox properties. These findings open up new perspectives for future research on dyes with advanced optical and redox properties. It also opens up new avenues of research, particularly in ophthalmic research, where panchromatic photochromic dyes are a requirement for light-adaptive lenses, or in research on semi-transparent solar cells, where CRI and AVT indices are of great interest.

Author contributions

D. M. synthesized and characterized the dyes. S. F. performed the synthesis of some intermediates. P. M. and D. M. performed the DFT calculations. J. P. performed X-ray diffraction analysis and refinements on single crystals. A. J. R. and D. M. fabricated and characterized the solar cells. R. D. and D. M. designed the materials and experiments. R. D. acquired the funding and supervised the work with the help of C. A. R. D. and D. M. treated the data and wrote the manuscript, with contributions from all authors. All authors have given approval to the final version of the manuscript.

Conflicts of interest

There are no conflicts to declare.

Data availability

All data supporting the findings of this study are provided in the SI. This includes theoretical calculations, synthetic procedures, crystallographic data, NMR spectra of intermediates and final compounds, optical measurements, cyclic voltammetry measurements, and details regarding the preparation and

characterization of the polymeric matrix. Crystallographic data for compounds [Prec1, 1, 3, 8, 9, 10, 11, 12, and 13] have been deposited with the Cambridge Crystallographic Data Centre (CCDC) under deposition numbers 2455765–2455773. The raw data supporting the conclusions of this article are available from the corresponding authors upon reasonable request.

Theoretical calculations, synthetic procedures, crystallographic data, NMR spectra, details on optical measurements, CRI and AVT determination, cyclic voltammetry, polymeric matrix preparation and characterization, solar cell fabrication and characterization, as well as additional figures. See DOI: **https://doi.org/10.1039/d5qm00412h**

CCDC 2455765–2455773 contain the supplementary crystallographic data for this paper.[76–84]

Acknowledgements

P. M. thanks GENCI (CINES and IDRIS) for high-performance computing resources (grant 2019-A0060807648). R. D. acknowledges the European Research Council (ERC) for funding. This project has received funding under the European Union's Horizon 2020 research and innovation program (grant agreement number 832606; project PISCO).

Notes and references

1 B. Wardle, *Principles and Applications of Photochemistry*, John Wiley & Sons, 2009.
2 S. Molla and S. Bandyopadhyay, Visible light mediated efficient photoswitching of dimethyldihydropyrenes in thin films for all-photonic logic gate applications and dynamic encryption/decryption capabilities, *J. Mater. Chem. C*, 2024, **12**, 17511–17518.
3 G. Berkovic, V. Krongauz and V. Weiss, Spiropyrans and Spirooxazines for Memories and Switches, *Chem. Rev.*, 2000, **100**, 1741–1754.
4 S. Kawata and Y. Kawata, Three-Dimensional Optical Data Storage Using Photochromic Materials, *Chem. Rev.*, 2000, **100**, 1777–1788.
5 D. Alcer, N. Zaiats, T. K. Jensen, A. M. Philip, E. Gkanias, N. Ceberg, A. Das, V. Flodgren, S. Heinze, M. T. Borgström, B. Webb, B. W. Laursen and A. Mikkelsen, Integrating molecular photoswitch memory with nanoscale optoelectronics for neuromorphic computing, *Commun. Mater.*, 2025, **6**, 1–11.
6 W. Zhang, Y. Cheng, M. Wu and X. Xie, Photoswitchable chemical sensing based on the colorimetric pH response of ring-opened naphthopyrans, *Sens. Actuators, B*, 2024, **407**, 135475.
7 M. Qin, Y. Huang, F. Li and Y. Song, Photochromic sensors: a versatile approach for recognition and discrimination, *J. Mater. Chem. C*, 2015, **3**, 9265–9275.
8 Y. Zhuge, D. Xu, C. Zheng and S. Pu, An ionic liquid-modified diarylethene: synthesis, properties and sensing cyanide ions, *Anal. Chim. Acta*, 2019, **1079**, 153–163.
9 Y. Ke, J. Chen, G. Lin, S. Wang, Y. Zhou, J. Yin, P. S. Lee and Y. Long, Smart Windows: Electro-, Thermo-, Mechano-, Photochromics, and Beyond, *Adv. Energy Mater.*, 2019, **9**, 1902066.
10 Y. Wang, E. L. Runnerstrom and D. J. Milliron, Switchable Materials for Smart Windows, *Annu. Rev. Chem. Biomol. Eng.*, 2016, **7**, 283–304.
11 M. Irie, T. Fukaminato, K. Matsuda and S. Kobatake, Photochromism of Diarylethene Molecules and Crystals: Memories, Switches, and Actuators, *Chem. Rev.*, 2014, **114**, 12174–12277.
12 M. Mennig, K. Fries, M. Lindenstruth and H. Schmidt, Development of fast switching photochromic coatings on transparent plastics and glass, *Thin Solid Films*, 1999, **351**, 230–234.
13 Z. Wu, L. Xiao, K. Liao, J. Liu, Q. Zou, W. Wang, M. Gong and G. Wang, Light-responsive spiropyran derivative with tunable assembly morphology and solid-state photochromism for rewritable optical printing and multi-level anti-counterfeiting, *J. Mater. Chem. C*, 2024, **12**, 17935–17942.
14 A. Abdollahi, H. Roghani-Mamaqani, B. Razavi and M. Salami-Kalajahi, Photoluminescent and Chromic Nanomaterials for Anticounterfeiting Technologies: Recent Advances and Future Challenges, *ACS Nano*, 2020, **14**, 14417–14492.
15 S. Nigel Corns, S. M. Partington and A. D. Towns, Industrial organic photochromic dyes, *Color. Technol.*, 2009, **125**, 249–261.
16 J. C. Crano, T. Flood, D. Knowles, A. Kumar and B. V. Gemert, Photochromic compounds: chemistry and application in ophthalmic lenses, *Pure Appl. Chem.*, 1996, **68**, 1395–1398.
17 R. A. Evans, T. L. Hanley, M. A. Skidmore, T. P. Davis, G. K. Such, L. H. Yee, G. E. Ball and D. A. Lewis, The generic enhancement of photochromic dye switching speeds in a rigid polymer matrix, *Nat. Mater.*, 2005, **4**, 249–253.
18 B.-K. Kim, J. Deng, W. Xiao, B. V. Gemert, A. Chopra, F. Molock and S. Mahadevan, *United States*, *Ophthalmic devices comprising photochromic materials having extended PI-conjugated systems*, US20060226402A1, 2006.
19 K.-H. Cheng, T.-L. Hsieh, S.-J. Liu, C.-J. Chiang and J.-C. Chen, Synthesis and characterization of indeno-fused naphthopyrans containing methacryloyl and urethane groups for photochromic contact lenses applications, *Eur. Polym. J.*, 2024, **211**, 113044.
20 W. Luo, J. M. A. Castán, D. Mirani, A. J. Riquelme, A. K. Sachan, O. Kurman, S. Kim, F. Faini, P. Zimmermann, A. Hinderhofer, Y. Patel, A. T. Frei, J.-E. Moser, D. Ramirez, F. Schreiber, P. Maldivi, J.-Y. Seo, W. Tress, G. Grancini, R. Demadrille and J. V. Milić, Photochromic Control in Hybrid Perovskite Photovoltaics, *Adv. Mater.*, 2025, **37**, 2420143.
21 Q. Huaulmé, V. M. Mwalukuku, D. Joly, J. Liotier, Y. Kervella, P. Maldivi, S. Narbey, F. Oswald, A. J. Riquelme, J. A. Anta and R. Demadrille, Photochromic dye-sensitized solar cells with light-driven adjustable optical transmission and power conversion efficiency, *Nat. Energy*, 2020, **5**, 468–477.

22 V. M. Mwalukuku, J. Liotier, A. J. Riquelme, Y. Kervella, Q. Huaulmé, A. Haurez, S. Narbey, J. A. Anta and R. Demadrille, Strategies to Improve the Photochromic Properties and Photovoltaic Performances of Naphthopyran Dyes in Dye-Sensitized Solar Cells, *Adv. Energy Mater.*, 2023, **13**, 2203651.
23 T. Tsujioka and M. Irie, Electrical functions of photochromic molecules, *J. Photochem. Photobiol., C*, 2010, **11**, 1–14.
24 Z. Li, X. Zeng, C. Gao, J. Song, F. He, T. He, H. Guo and J. Yin, Photoswitchable diarylethenes: from molecular structures to biological applications, *Coord. Chem. Rev.*, 2023, **497**, 215451.
25 Y. Yokoyama, Fulgides for Memories and Switches, *Chem. Rev.*, 2000, **100**, 1717–1740.
26 F. A. Jerca, V. V. Jerca and R. Hoogenboom, Advances and opportunities in the exciting world of azobenzenes, *Nat. Rev. Chem.*, 2022, **6**, 51–69.
27 H. M. Dhammika Bandara and S. C. Burdette, Photoisomerization in different classes of azobenzene, *Chem. Soc. Rev.*, 2012, **41**, 1809–1825.
28 L. Kortekaas and W. R. Browne, The evolution of spiropyran: fundamentals and progress of an extraordinarily versatile photochrome, *Chem. Soc. Rev.*, 2019, **48**, 3406–3424.
29 A. Towns, Naphthopyran Dyes, *Phys. Sci. Rev.*, 2020, **5**, 20190085.
30 M. E. McFadden, R. W. Barber, A. C. Overholts and M. J. Robb, Naphthopyran molecular switches and their emergent mechanochemical reactivity, *Chem. Sci.*, 2023, **14**, 10041–10067.
31 V. Graça, J. Berthet, S. Delbaere and P. J. Coelho, Photochromism of 2*H*-naphtho[1,2-*b*]pyran-4-carboxylates, *Dyes Pigm.*, 2023, **212**, 111130.
32 Z. Xu, J. Sun, T. Yan, H. Zhang and J. Han, Silindeno-fused 3*H*-naphthopyrans with fast thermal fading rate and high optical density, *J. Mater. Chem. C*, 2024, **12**, 2961–2967.
33 H. Kuroiwa, Y. Inagaki, K. Mutoh and J. Abe, On-Demand Control of the Photochromic Properties of Naphthopyrans, *Adv. Mater.*, 2019, **31**, 1805661.
34 A. Mukhopadhyay, V. K. Maka and J. N. Moorthy, Remarkable Influence of Phenyl/Arylethynylation on the Photochromism of 2,2-Diphenylbenzopyrans (Chromenes), *Eur. J. Org. Chem.*, 2016, 274–281.
35 B. V. Gemert, The Commercialization of Plastic Photochromic Lenses: A Tribute to John Crano, *Mol. Cryst. Liq. Cryst. Sci. Technol., Sect. A*, 2000, **344**, 57–62.
36 R. Pardo, M. Zayat and D. Levy, Photochromic organic–inorganic hybrid materials, *Chem. Soc. Rev.*, 2011, **40**, 672–687.
37 N. Malic, J. A. Campbell, A. S. Ali, M. York, A. D'Souza and R. A. Evans, Controlling Molecular Mobility in Polymer Matrices: Synchronizing Switching Speeds of Multiple Photochromic Dyes, *Macromolecules*, 2010, **43**, 8488–8501.
38 D. A. Clarke, B. M. Heron, C. D. Gabbutt, J. D. Hepworth, S. M. Partington and S. N. Corns, *United States, Grey coloring photochromic fused pyrans*, US6387512B1, 2002.
39 D. A. Clarke, B. M. Heron, C. D. Gabbutt, J. D. Hepworth, S. M. Partington and S. N. Corns, *United States, Neutral coloring photochromic 2H-naphtho[1,2-b] pyrans and heterocyclic pyrans*, US6248264B1, 2001.
40 S. Anguille, P. Brun and R. Guglielmetti, NEW FERROCENYL-NAPHTHOPYRANS WITH ORIGINAL PHOTOCHROMIC BEHAVIOUR, *Heterocycl. Commun.*, 1998, **4**, 63–70.
41 S. Anguille, P. Brun, R. Guglielmetti, Y. P. Strokach, A. A. Ignatin, V. A. Barachevsky and M. V. Alfimov, Synthesis and photochromic properties of ferrocenyl substituted benzo- and dibenzochromenes, *J. Chem. Soc., Perkin Trans. 2*, 2001, 639–644.
42 P. Brun, R. Guglielmetti and S. Anguille, Metallocenyl-[2*H*]naphtho[1,2-*b*]pyrans: metal effect on the photochromic behaviour, *Appl. Organomet. Chem.*, 2002, **16**, 271–276.
43 M. Cariello, S. Ahn, K.-W. Park, S.-K. Chang, J. Hong and G. Cooke, An investigation of the role increasing π-conjugation has on the efficiency of dye-sensitized solar cells fabricated from ferrocene-based dyes, *RSC Adv.*, 2016, **6**, 9132–9138.
44 R. Chauhan, M. Trivedi, L. Bahadur and A. Kumar, Application of π-Extended Ferrocene with Varied Anchoring Groups as Photosensitizers in TiO2-Based Dye-Sensitized Solar Cells (DSSCs), *Chem. – Asian J.*, 2011, **6**, 1525–1532.
45 J. Kulhánek, F. Bureš, W. Kuznik, I. V. Kityk, T. Mikysek and A. Růžička, Ferrocene-Donor and 4,5-Dicyanoimidazole-Acceptor Moieties in Charge-Transfer Chromophores with π Linkers Tailored for Second-Order Nonlinear Optics, *Chem. – Asian J.*, 2013, **8**, 465–475.
46 J. Kulhánek, F. Bureš, J. Opršal, W. Kuznik, T. Mikysek and A. Růžička, 1,4-Phenylene and 2,5-Thienylene π-Linkers in Charge-Transfer Chromophores, *Asian J. Org. Chem.*, 2013, **2**, 422–431.
47 D. Sirbu, C. Turta, A. C. Benniston, F. Abou-Chahine, H. Lemmetyinen, N. V. Tkachenko, C. Wood and E. Gibson, Synthesis and properties of a meso-tris–ferrocene appended zinc(II) porphyrin and a critical evaluation of its dye sensitised solar cell (DSSC) performance, *RSC Adv.*, 2014, **4**, 22733–22742.
48 R. Misra, R. Maragani, K. R. Patel and G. D. Sharma, Synthesis, optical and electrochemical properties of new ferrocenyl substituted triphenylamine based donor–acceptor dyes for dye sensitized solar cells, *RSC Adv.*, 2014, **4**, 34904–34911.
49 R. Chauhan, S. Auvinen, A. S. Aditya, M. Trivedi, R. Prasad, M. Alatalo, D. P. Amalnerkar and A. Kumar, Light harvesting properties of ferrocenyl based sensitizer with sulfur rich dithiocarabamates and xanthate as anchoring group, *Sol. Energy*, 2014, **108**, 560–569.
50 R. Chauhan, M. Shahid, M. Trivedi, D. P. Amalnerkar and A. Kumar, Dye-Sensitized Solar Cells with Biferrocenyl Antennae Having Quinoxaline Spacers, *Eur. J. Inorg. Chem.*, 2015, 3700–3707.
51 R. Chauhan, R. Yadav, A. Kumar Singh, M. Trivedi, G. Kociok-Köhn, A. Kumar, S. Gosavi and S. Rane, Ferrocenyl chalcones with phenolic and pyridyl anchors as potential sensitizers in dye-sensitized solar cells, *RSC Adv.*, 2016, **6**, 97664–97675.
52 R. Maragani, R. Misra, M. S. Roy, M. Kumar Singh and G. D. Sharma, (D–π–A) 2–π–D–A type ferrocenyl bisthiazole

linked triphenylamine based molecular systems for DSSC: synthesis, experimental and theoretical performance studies, *Phys. Chem. Chem. Phys.*, 2017, **19**, 8925–8933.

53 R. Yadav, A. Singh, G. Kociok-Köhn, R. Chauhan, A. Kumar and S. Gosavi, Ferrocenyl benzimidazole with carboxylic and nitro anchors as potential sensitizers in dye-sensitized solar cells, *New J. Chem.*, 2017, **41**, 7312–7321.

54 A. Singh, P. Singh, G. Kociok-Köhn, M. Trivedi, A. Kumar, R. Chauhan, S. B. Rane, C. Terashima, S. W. Gosavi and A. Fujishima, 1,1′-Bis(diphenylphosphino)ferrocene-appended nickel(II) dithiolates as sensitizers in dye-sensitized solar cells, *New J. Chem.*, 2018, **42**, 9306–9316.

55 A. Singh, G. Kociok-Köhn, R. Chauhan, M. Muddassir, S. W. Gosavi and A. Kumar, Ferrocene Appended Asymmetric Sensitizers with Azine Spacers with phenolic/nitro anchors for Dye-Sensitized Solar Cells, *J. Mol. Struct.*, 2022, **1249**, 131630.

56 K. K. Chenab and M.-R. Zamani-Meymian, Developing efficient dye-sensitized solar cells by inclusion of ferrocene and benzene π-bridges into molecular structures of triphenylamine dyes, *Mater. Sci. Semicond. Process.*, 2022, **151**, 107018.

57 S. Prabu, T. Viswanathan, E. David, S. Jagadeeswari and N. Palanisami, Enhancement of photovoltaic performance in ferrocenyl π-extended multi donor–π–acceptor (D–D′–π–A) dyes using chenodeoxycholic acid as a dye co-adsorbent for dye sensitized solar cells, *RSC Adv.*, 2023, **13**, 9761–9772.

58 T. Daeneke, T.-H. Kwon, A. B. Holmes, N. W. Duffy, U. Bach and L. Spiccia, High-efficiency dye-sensitized solar cells with ferrocene-based electrolytes, *Nat. Chem.*, 2011, **3**, 211–215.

59 T. Daeneke, A. J. Mozer, T.-H. Kwon, N. W. Duffy, A. B. Holmes, U. Bach and L. Spiccia, Dye regeneration and charge recombination in dye-sensitized solar cells with ferrocene derivatives as redox mediators, *Energy Environ. Sci.*, 2012, **5**, 7090–7099.

60 R. Wei, R. Zhou, R. Shen and J. Han, Tuning the photochromism of indeno-fused 2*H*-naphthopyrans using steric spirocyclic groups, *New J. Chem.*, 2024, **48**, 15352–15357.

61 P. J. Coelho, C. J. R. Silva, C. Sousa and S. D. F. C. Moreira, Fast and fully reversible photochromic performance of hybrid sol–gel films doped with a fused-naphthopyran, *J. Mater. Chem. C*, 2013, **1**, 5387–5394.

62 E. Rauzy, C. Berro, S. Morel, G. Herbette, V. Lazzeri and R. Guglielmetti, Modelling of the interactions between a photochromic naphthopyran and a poly(methyl methacrylate) matrix through the variation of the glass transition temperature and application of the energy/volume/mass (EVM) model, *Polym. Int.*, 2004, **53**, 455–459.

63 G. Favaro, F. Ortica, A. Romani and P. Smimmo, Photochromic behaviour of Berry Red studied in solution and polymer films, *J. Photochem. Photobiol., C*, 2008, **196**, 190–196.

64 M. R. di Nunzio, P. L. Gentili, A. Romani and G. Favaro, Photochromism and Thermochromism of some Spirooxazines and Naphthopyrans in the Solid State and in Polymeric Film, *J. Phys. Chem. C*, 2010, **114**, 6123–6131.

65 J. Zou, J. Liao, Y. He, T. Zhang, Y. Xiao, H. Wang, M. Shen, T. Yu and W. Huang, Recent Development of Photochromic Polymer Systems: Mechanism, Materials, and Applications, *Research*, 2024, **7**, 0392.

66 S. Fauvel, A. J. Riquelme, J.-M. A. Castán, V. Mwatati Mwalukuku, Y. Kervella, V. Kumar Challuri, F. Sauvage, S. Narbey, P. Maldivi, C. Aumaître and R. Demadrille, Push-pull photochromic dyes for semi-transparent solar cells with light-adjustable optical properties and high color-rendering index, *Chem. Sci.*, 2023, **14**, 8497–8506.

67 J. Liotier, V. M. Mwalukuku, S. Fauvel, A. J. Riquelme, J. A. Anta, P. Maldivi and R. Demadrille, Photochromic Naphthopyran Dyes Incorporating a Benzene, Thiophene, or Furan Spacer: Effect on Photochromic, Optoelectronic, and Photovoltaic Properties in Dye-Sensitized Solar Cells, *Sol. RRL*, 2022, **6**, 2100929.

68 L. Zhang and J. M. Cole, Anchoring Groups for Dye-Sensitized Solar Cells, *ACS Appl. Mater. Interfaces*, 2015, **7**, 3427–3455.

69 Masud and H. K. Kim, Redox Shuttle-Based Electrolytes for Dye-Sensitized Solar Cells: Comprehensive Guidance, Recent Progress, and Future Perspective, *ACS Omega*, 2023, **8**, 6139–6163.

70 G. Turkoglu, M. E. Cinar and T. Ozturk, in *Sulfur Chemistry*, ed. X. Jiang, Springer International Publishing, Cham, 2019, pp. 79–123.

71 B. Luccioni-Houzé, M. Campredon, R. Guglielmetti and G. Giusti, Kinetic Analysis of Fluoro-[2*H*]-Chromenes at the Photostationary States, *Mol. Cryst. Liq. Cryst. Sci. Technol., Sect. A*, 1997, **297**, 161–165.

72 R. Demadrille, A. Rabourdin, M. Campredon and G. Giusti, Spectroscopic characterisation and photodegradation studies of photochromic spiro[fluorene-9,3′-[3′*H*]-naphtho[2,1-*b*]pyrans], *J. Photochem. Photobiol., C*, 2004, **168**, 143–152.

73 J.-S. Lin, Interaction between dispersed photochromic compound and polymer matrix, *Eur. Polym. J.*, 2003, **39**, 1693–1700.

74 P. F. de Violet and S. R. Logan, Mechanism of the photochemical reaction between ferrocene and iodine, *J. Chem. Soc., Faraday Trans. 1*, 1980, **76**, 578.

75 A. M. El-Zohry, J. Cong, M. Karlsson, L. Kloo and B. Zietz, Ferrocene as a rapid charge regenerator in dye-sensitized solar cells, *Dyes Pigm.*, 2016, **132**, 360–368.

76 D. Mirani, A. J. Riquelme, S. Fauvel, C. Aumaître, P. Maldivi, J. Pécaut and R. Demadrille, CCDC 2455765: Experimental Crystal Structure Determination, 2025, DOI: **10.5517/ccdc.csd.cc2nff7s**.

77 D. Mirani, A. J. Riquelme, S. Fauvel, C. Aumaître, P. Maldivi, J. Pécaut and R. Demadrille, CCDC 2455766: Experimental Crystal Structure Determination, 2025, DOI: **10.5517/ccdc.csd.cc2nff8t**.

78 D. Mirani, A. J. Riquelme, S. Fauvel, C. Aumaître, P. Maldivi, J. Pécaut and R. Demadrille, CCDC 2455767: Experimental Crystal Structure Determination, 2025, DOI: **10.5517/ccdc.csd.cc2nff9v**.

79 D. Mirani, A. J. Riquelme, S. Fauvel, C. Aumaître, P. Maldivi, J. Pécaut and R. Demadrille, CCDC 2455768: Experimental

Crystal Structure Determination, 2025, DOI: 10.5517/ccdc.csd.cc2nffbw.
80 D. Mirani, A. J. Riquelme, S. Fauvel, C. Aumaître, P. Maldivi, J. Pécaut and R. Demadrille, CCDC 2455769: Experimental Crystal Structure Determination, 2025, DOI: 10.5517/ccdc.csd.cc2nffcx.
81 D. Mirani, A. J. Riquelme, S. Fauvel, C. Aumaître, P. Maldivi, J. Pécaut and R. Demadrille, CCDC 2455770: Experimental Crystal Structure Determination, 2025, DOI: 10.5517/ccdc.csd.cc2nffdy.
82 D. Mirani, A. J. Riquelme, S. Fauvel, C. Aumaître, P. Maldivi, J. Pécaut and R. Demadrille, CCDC 2455771: Experimental Crystal Structure Determination, 2025, DOI: 10.5517/ccdc.csd.cc2nfffz.
83 D. Mirani, A. J. Riquelme, S. Fauvel, C. Aumaître, P. Maldivi, J. Pécaut and R. Demadrille, CCDC 2455772: Experimental Crystal Structure Determination, 2025, DOI: 10.5517/ccdc.csd.cc2nffg0.
84 D. Mirani, A. J. Riquelme, S. Fauvel, C. Aumaître, P. Maldivi, J. Pécaut and R. Demadrille, CCDC 2455773: Experimental Crystal Structure Determination, 2025, DOI: 10.5517/ccdc.csd.cc2nffh1.